Experimental investigation on porosity of carbon fiber-reinforced composite using ultrasonic attenuation coefficient

L. LIN [1*], M. LUO [2], H. T. TIAN [1], X. M. LI [1], G. P. GUO [3]

[1]NDT & E Laboratory, School of Materials Science & Engineering, Dalian University of Technology, Dalian 116024, China

[2]Beijing Aerospace Research Institute of Materials and Processing Technology, Beijing, 100076, China

[3]Beijing Institute of Aeronautic Materials, Beijing, 100095, China

[*] Corresponding author: Tel 86-411-84707117; Fax 86-411-84709284; E-mail：linli@dlut.edu.cn (L. LIN)

Abstract The present work experimentally investigates the correlations between ultrasonic attenuation coefficient and void content with the porosity 0.03%-4.96% of the carbon fiber-reinforced composite (CFRC) samples. The ultrasonic echo immersion bottom reflection technique with 5MHz flat probe is adopted to determine the attenuation coefficient and the metallographic microscope is used to measure the porosity destructively. A linear and a parabolic curve are found to be suitable to fit the data with the porosity 0.03%-0.5% and 0.5%-4.96%, respectively. It is observed that ultrasonic predictions accord with the microscopic results. The present data have been compared with the known testing models and empirical formulas. The power law between the attenuation coefficient and the porosity, the critical porosity phenomenon, and the effects of void morphology on ultrasonic attenuation have been discussed. This work not only provides experimental evidence in making clear the ultrasonic attenuation mechanism of pores, but also further proves that the attenuation coefficient could be used to nondestructively characterize the void content in composites.

Keywords carbon fiber-reinforced composite; porosity; ultrasonic testing; attenuation coefficient

1 INTRODUCTION

CFRC materials are used more and more in aircraft industry due to their high rigidity and their relatively low weight. Low porosity levels are essential for ensuring the performance of the CFRC structures [1-3]. Effective works to ultrasonically determine the void content of composite have been made based on the correlations between the porosity and the attenuation coefficient [4-11], velocity [12-13] or back-scatter [14-15], respectively. Using attenuation coefficient to determine the porosity levels seems convenient and effective. Many attempts have been made to improve the theory analysis and experiment techniques.

The correlation in theory between the porosity and the attenuation coefficient is easy to understand and the dependence of the two parameters has been observed experimentally. However, the attenuation mechanism of pores is still not clear in principle of physics and the universally accepted theory and test model have not been established. Especially for the porosity below 2.5%, the maximum allowed for most advanced CFRC in aerospace applications, experimental investigations are very limited, which have hindered people from understanding the attenuation mechanism of void well. For example, According to Stone and Clarkes' report [4], a bi-linear empirical formula was established with the critical porosity 1.5%. An early assumption proposed by

Martin suggested that the voids were spherical, had the same dimension and distributed symmetrically [5]. The later research by Hale and Ashton [6] improved Martin's model by supposing the voids to be spherical or discal and the dimension had different distribution rules. However, when they verified the ultrasonic experiment results by using microscopic technique, limited samples were provided. Although it seems that the porosity data covered the range from 1% to 5%, "blind spot" even "blind area" appeared since the porosity data were much dispersed, which weakened the effectiveness of verification of ultrasonic techniques.

In the present work, ultrasonic attenuation inspection and metallographic microscope observation are investigated for 17 composite sample plates with the porosity 0.03%-4.96%. It is particularly important to note that, among them, the porosity of 11 samples is lower than 2.5%. Based on the ultrasonic echo immersion bottom reflection technique, the attenuation coefficient is determined and the empirical formula between the attenuation coefficient and the porosity is established according to the microscopic results. It has been observed that there is a critical porosity phenomenon. According to the porosity lower or higher than the critical value, the rules of the attenuation coefficient as a function of the porosity are various. This phenomenon probably implies that the scattering attenuation mechanisms of pores rely on the variation of porosity. Moreover, some opinions are further proposed about the understanding of ultrasonic attenuation of pores in composites.

2. EXPERIMENTS

2.1 Samples

A series of 16-layered press molding unidirectional enhanced carbon fiber-epoxy composite plates were investigated. The samples were prepared by hand paste molding craft. The thickness of the composite panels is 2±0.05mm, the area more than 200×250mm^2 and the fiber content is 69±3%. Firstly the testing areas were pre-selected according to the amplitude of the ultrasonic echo, and then scanned using ultrasonic C-scan equipment to choose the regions with uniform distribution of pores.

2.2 Ultrasonic method and experiment

The attenuation coefficient is measured using ultrasonic echo immersion bottom reflection technique, as shown in Fig.1. Acting as a flat smooth surface, a glass sheet is placed at the tank bottom. With this method, the testing sensitivity is enhanced due to the wave's double penetrations through the sample. Moreover, the back echoes from the sample and the tank bottom are separated easily due to the existence of the glass. The excitation, observation and collection of the ultrasonic signal are fulfilled by GE USIP40 ultrasonic flaw detector. A flat immersion probe with the frequency 5 MHz is used in the testing. Through comparing the acoustical pressure whether there is a sample or not, the attenuation coefficient of the composite sample could be deduced.

The incident pressure is noted as P_0. The sample thickness is written as d_s; d_{w1} is the distance from the transducer to the front surface of the sample; d_{w2} is the distance from the sample back surface to the front surface of the glass sheet. The subscripts "w", "s" and "g"

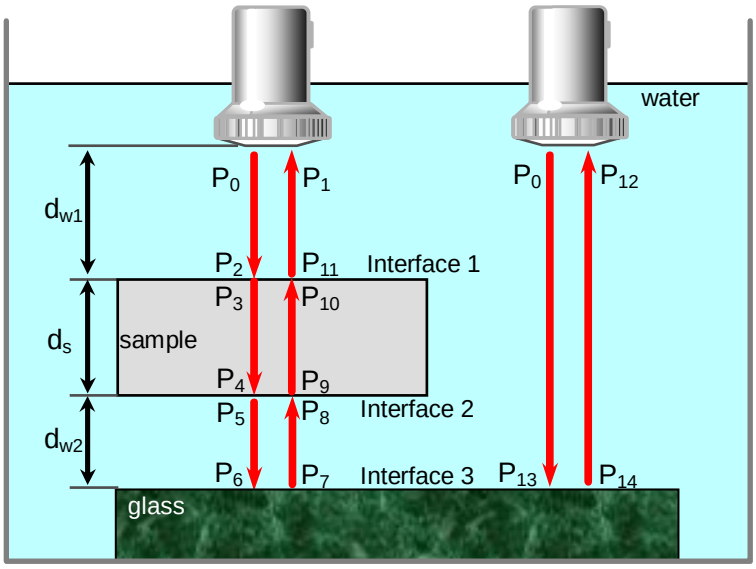

Figure 1. Experimental setup for attenuation coefficient measurement

refer to the water, sample and glass, respectively, α is attenuation coefficient, *c* is longitudinal velocity, ρ is density, T and R refer to the transmission coefficient and reflection coefficient, respectively, the subscripts "1", "2" and "3" refer to the interface 1, 2 or 3. The other acoustical pressure parameters are shown in Fig. 1.

When there is a sample between the transducer and the glass sheet, a series of equations could be given:

$$\left.\begin{aligned}
P_2 &= P_0 \cdot e^{-\alpha_w d_{w1}} \\
P_3 &= P_2 \cdot T_1 \\
P_4 &= P_3 \cdot e^{-\alpha_s d_s} \\
P_5 &= P_4 \cdot T_2 \\
P_6 &= P_5 \cdot e^{-\alpha_w d_{w2}} \\
P_7 &= P_6 \cdot R_3 \\
P_8 &= P_7 \cdot e^{-\alpha_w d_{w2}} \\
P_9 &= P_8 \cdot T_1 \\
P_{10} &= P_9 \cdot e^{-\alpha_s d_s} \\
P_{11} &= P_{10} \cdot T_2 \\
P_1 &= P_{11} \cdot e^{-\alpha_w d_{w1}}
\end{aligned}\right\} \quad (1)$$

so we obtain

$$P_1 = P_0 R_3 T_1^2 T_2^2 e^{-2(\alpha_w d_{w1} + \alpha_s d_s + \alpha_w d_{w2})} \quad (2)$$

For the situation that there is no sample between the transducer and the glass sheet, similarly we obtain

$$P_{12} = P_0 R_3 e^{-2\alpha_w (d_{w1} + d_s + d_{w2})} \quad (3)$$

where

$$\left.\begin{aligned} T_1 &= \frac{2Z_s}{Z_s + Z_w} = \frac{2\rho_s c_s}{\rho_s c_s + \rho_w c_w} \\ T_2 &= \frac{2Z_w}{Z_s + Z_w} = \frac{2\rho_w c_w}{\rho_s c_s + \rho_w c_w} \\ R_3 &= \frac{Z_g - Z_w}{Z_g + Z_w} = \frac{\rho_g c_g - \rho_w c_w}{\rho_g c_g + \rho_w c_w} \end{aligned}\right\} \quad (4)$$

According to Eqs. (2) and (3), the following relation could be deduced

$$\frac{P_{12}}{P_1} = \frac{1}{T_1^2 T_2^2} e^{2d_S(\alpha_S - \alpha_W)} \quad (5)$$

Assume the amplitude of P_{12} and P_1 are written as A_{12} and A_1, respectively, then

$$\frac{A_{12}}{A_1} = \frac{1}{T_1^2 T_2^2} e^{2d_S(\alpha_S - \alpha_W)} \quad (6)$$

and

$$\alpha_s = \{\frac{10}{d_s}\lg\frac{A_{12}}{A_1} + \frac{20}{d_s}\lg(1 - R_1^2)\} + \alpha_w \quad (7)$$

where, α_w, and d_s are known; A_{12} and A_1 can be read from the ultrasonic detector directly. If the density of the composite sample with different porosities is looked as a constant, which could be measured in advance, R_1 could be obtained. Thus, α_c is easily determined according to Eq. (7).

2.3 Microscopic observation

Tested with ultrasonic technique, the surfaces of samples were grinded to no obvious scratches using 600# to 1500# sandpaper, then polished using flannel and polishing paste with particle size of 1.5μm until no microscopic scratch. GE Lycra MeF4A metallographic microscope was used to observe the sample cross-sectional. For each sample, some visions were observed for void statistics, the area void content was recorded and photographs were taken for the visions. In order to avoid the influence of void area in different cross sections, the sample thickness was grinded about 0.4 mm after each observation. The grinding was repeated more than 20 times until the whole sample was grinded out. According to the statistical theory, the volume porosity can be converted from the series of obtained area porosities [16]. Fig. 2 shows a group of typical microscopic observation results for porosity samples.

3. RESULTS AND DISCUSSION

3.1 Results

Fig. 3 presents the attenuation coefficient as a function of porosity. The attenuation coefficient is about 1.60dB/mm when no void, which is caused by the resin and fiber in composite material. The attenuation coefficient rises gradually with the enhancement of porosity from 0.03%. However, a critical value 1.5% was noticed, around which the correlation between the attenuation coefficient and porosity is different. A linear

approximation of the α evolution with P has been plotted for 0.30%-0.5%, while for 0.5%-4.96%, a second order polynomial approximation plotted according to the following equations:

$$\left.\begin{array}{ll} \alpha=a+bP & (0.03\% \le P \le 0.5\%) \\ \alpha=c_1+c_2P+c_3P^2 & (0.5\% < P \le 4.96\%) \end{array}\right\} \quad (8)$$

where a, b, c_1, c_2 and c_3 are constants for given frequency, which could be determined according to the experimental calibration on reference samples without void. The attenuation coefficient as a function of porosity could be determined using the following equation:

$$\left.\begin{array}{ll} \alpha=1.65+1.78P & (0.03\% \le P \le 0.5\%) \\ \alpha=2.5+0.15P^2 & (0.5\% < P \le 4.96\%) \end{array}\right\} \quad (9)$$

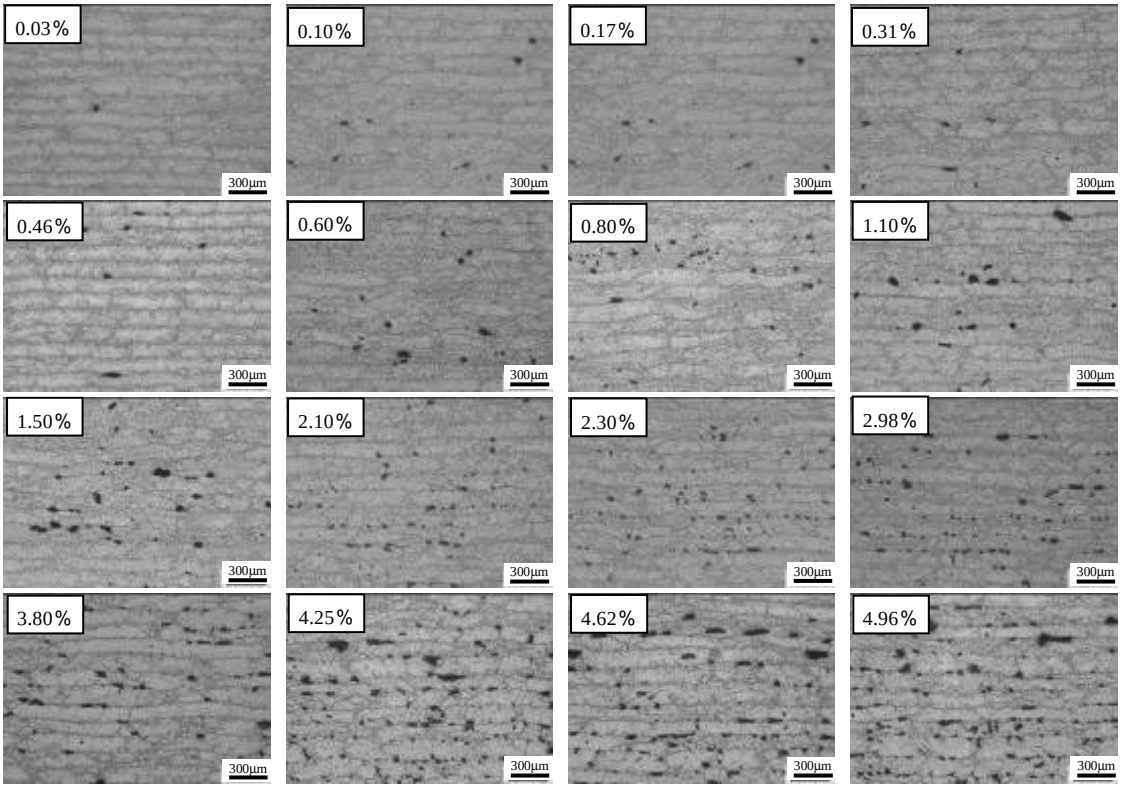

Figure 2. Typical metallographic images of the composite samples with different porosity

3.2 Error analysis

To verifying the ultrasonic determination results, different pores areas for the same batch of composite material samples is inspected. Fig. 4 shows the porosity results from empirical formula (9) and metallographic microscopic observation. With the porosity changing from 0.03% to 2.21%, it is found that the ultrasonic estimations basically accord with that of microscopic determinations.

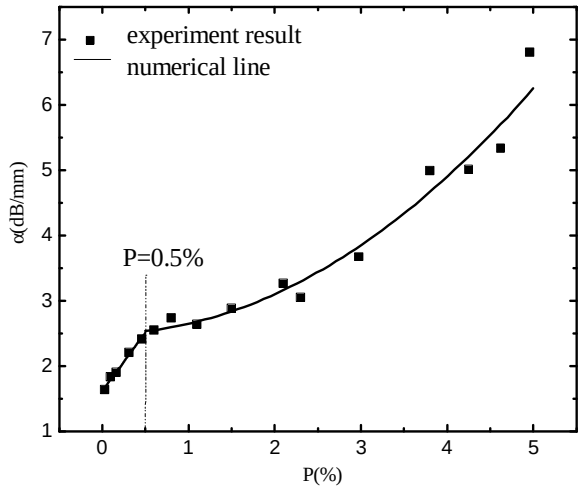

Figure 3. The relation between the ultrasonic attenuation coefficient and the porosity

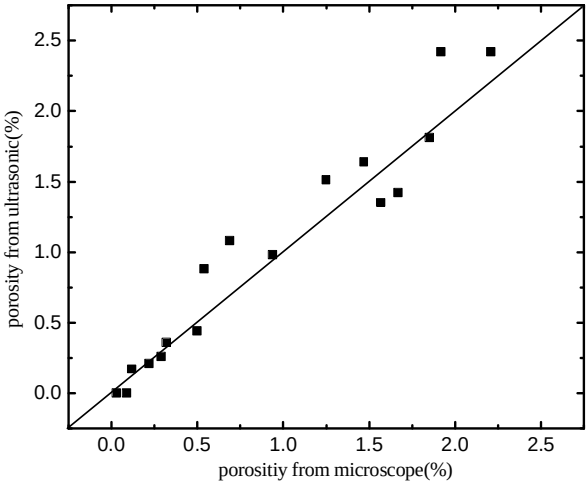

Figure 4. The comparison of the porosity between ultrasonic and metallographic methods

In Fig. 5, we present the relative error analysis of porosity results. It is noticed that most error are lower than 25%. Obvious derivations occur in three small porosity samples, such as 0.03% 0.09% and 0.12%, and the porosity 0.54% and 0.69%. There are may be two reasons for explaining these disagreements. Firstly, it is difficult to ensure that the ultrasonic testing area does not deviate from the location of metallographic observation. Secondly, the shape, size, and distribution of pores are random in a whole, which may cause some fluctuation of ultrasonic attenuation.

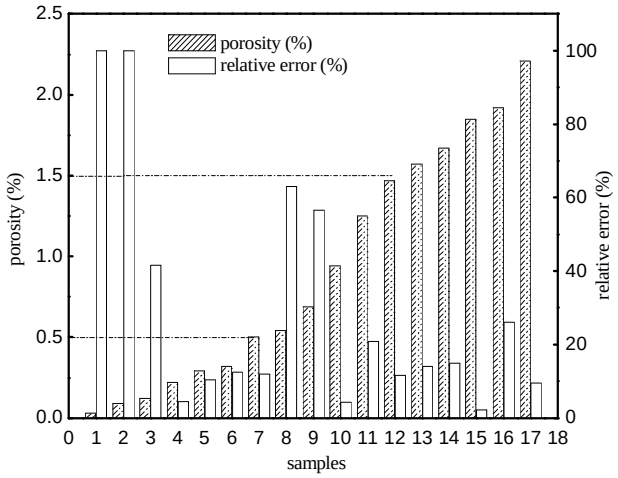

Figure 5. The error analysis of the ultrasonic testing results of porosity

3.3 Discussion

Ever since the first report of the ultrasonic estimation of porosity for composites with

attenuation coefficient by Stone and Clarke, the relation between the porosity and the attenuation coefficient has attracted much attention. Based on the elastic theory for isotropic and homogeneous media contain voids proposed by Hashin [17], some test models have been established and empirical formulas are provided. However, appropriate explanation for the ultrasonic experimental results has not been proposed. In order to make clear the attenuation mechanism of pores in composites, some important points more than the empirical formula itself should be paid more attention.

Comprehensively considering most of the testing models and empirical formulas, the attenuation coefficient as a function of porosity could be given like this:

$$\alpha=AP^m+BP^n \tag{10}$$

where *A* is the attenuation constant including fiber, resin substrate, etc; *B* is a function of testing frequency, as well as shape, size, and distribution of voids. *n* means the power. In general, *n* changes among 1-3.

(1) For the same samples, the various empirical formulas may show minor differences for the determination of the porosity.

In our case, other two empirical formulas have been given to compare with the equation (9):

$$\alpha_1=0.5+2.5P^2 \tag{11}$$

$$\alpha_2=2.74+0.26P+0.2P^2 \tag{12}$$

Despite the expression and the parameters are different, it is found that there are no obvious differences among the three numerical fitting results except (Fig. 6). Birt and Smith [3] compared two fitting results of porosity testing from Stone using parabola and bi-linear relation, respectively. Although it seems that bi-linear fitting results have better agreement with experimental data, the difference between each other is also small. It is inferred that neither the expression nor the value of the fitting parameters is very important in nature for developing the ultrasonic attenuation mechanism.

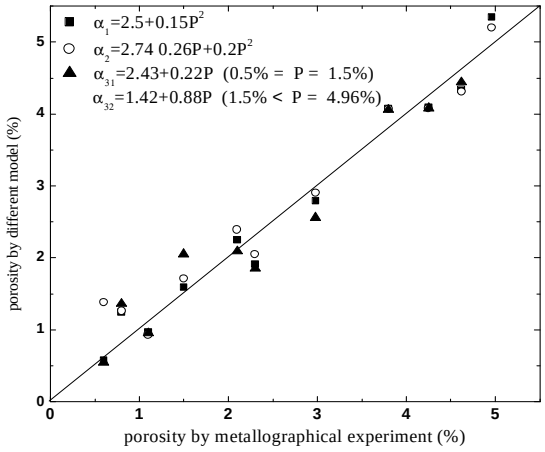

Fig. 6 The comparison of porosity obtained by three model and metallographic analysis

(2) The critical porosity phenomenon may imply some transformation of ultrasonic attenuation mechanism of void.

For example, Stone and Clarke observed the “critical porosity”, They found that when the porosity was less than 1.5%, voids were mainly spherical and their diameters were around $5 \sim 20\mu m$. When the porosity is more than 1.5%, most voids tended to become flat and dimensions became larger. The bi-linear fitting results further indicate the inference of affections from the random change of morphology of pores. In our case, similar phenomenon has also been observed. The critical porosity value is 0.5%, however, not 1.5%, which maybe resulted from the different samples preparations. Stone assumed that various origins of voids may explain the critical porosity phenomenon. Despite it is not very clear how the ultrasonic wave propagates and attenuates in the composites containing pores, it is certain that the critical porosity phenomenon is not accidental. The attenuation mechanism of voids needs to be further investigated.

(3) More attention should be paid on the roles of morphology of pores when the test model is established.

The influence on attenuation caused by the size, shape and distribution of voids may be much larger than the current estimation. Fig. 7 shows comparisons of the attenuation coefficient as a function of porosity from Stone and Clarke’s (Line 1), Zhou’s (Line 2) and ours (Line 3). For the three cases, in general, the bigger the porosity is, the bigger the attenuation coefficient is. It is important to note that, however, the increasing rate from Lines 1 and 3 is different. With Line 3, the attenuation as a function of porosity seems increase progressively. Moreover, the Line 2 with the frequency 2.5MHz is also compared, which appears to be “parallel” to Line 3. However, for the same porosity, the values of attenuation coefficient are down 0.7 to 0.8dB/mm than Line 3, which is due to the high frequency corresponding to serious scattering energy loss. It is inferred that the size, shape, and distribution of voids attribute to the attenuation in some ways since same porosity shows different attenuation coefficient. David [18] and Hua et al [10] found that the size of voids increased with the rising of the porosity. The bigger porosity is, the smaller width-to-length ratio is. In contrast, smaller porosity corresponded to bigger width-to-length ratio. In addition, the voids tended to join together when they were thin and the shape of voids trended to

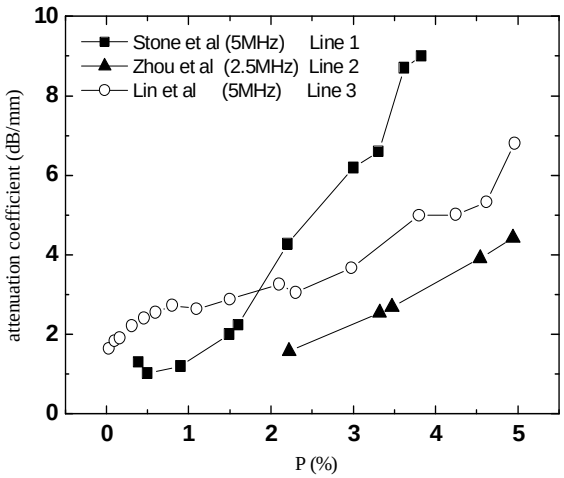

Fig.7 Comparisons of attenuation coefficient as a function of porosity

circular and the distribution was relatively scattered for low porosity. Considering the morphological characteristics is of great importance.

4 CONCLUSIONS

This paper investigated the porosity estimation technique using ultrasonic attenuation coefficient with low porosity for CFRC. The empirical formula between ultrasonic attenuation coefficient and void content has been established and validated. Based on the testing models and formulas, some opinions are further proposed about the understanding of ultrasonic attenuation of pores in composites. First, the form of the empirical formula is not uniquely important when the experimental porosity data are numerical fitted. Then, the critical porosity phenomenon may imply some transformation of ultrasonic attenuation mechanism related to the morphology of pores. Finally, it is of great importance to pay more attention to the roles of morphological characteristics of voids when ultrasonically determining the porosity using attenuation coefficient.

REFERENCES

[1] D.J. Hagemaier and R.H. Fassbender, Mater. Eval. 37 (1979) 43.
[2] U. Schnars and R. Henrich, http://www.ndt.net/article/cdcm2006/papers/schnars.pdf.
[3] E.A. Birt and R.A. Smith, Insight. 46 (2004) 681.
[4] D.E. Stone and B. Clarke, Nondestruct. Test. 8 (1975) 137.
[5] B.G. Martin, Nondestruct. Test. Int. 9 (1976) 242.
[6] J.M. Hale and J.N. Ashton, Nondestruct. Test. Int. 21(1988) 321.
[7] H. Jeong and D. K. Hsu, Ultrasonics. 33(1995) 195
[8] D. K. Hsu and S. M. Nair, Rev. Prog. Quant. Nondestruct. Eval. 6B (1986) 1185.
[9] D. K. Hsu. Rev. Prog. Quant. Nondestruct. Eval. 7B (1988) 1063.
[10] Z. H. Hua, X. J. Zhou and J. Z. Liu, Acta Mater. Compos. Sinica 14 (1997) 99.
[11] X. J. Zhou, J. Q. Mo, Acta Mater. Compos. Sinica, 14 (1997) 107.
[12] B. G. Martin, J. Appl. Phys. 48 (1977) 3368.
[13] W. N. Reynolds and S. J. Wilkinson, Ultrasonics. 16 (1978) 159.
[14] R. A. Robert, Rev. Prog. Quant. Nondestruct. Eval. 6B (1987) 1147.
[15] D. Grolemund and C. S. Tsai, IEEE Trans on Ultrasonics ferroelectrics and frequency control, 45(1998) 295.
[16] I. M. Daniel, S. C. Wooh and I. Komsky, Nondestruct. Eval. 11 (1992) 1.
[17] Z. Hashin, J. Appl. Mech. 29 (1962) 143.
[18] K. H. David and M. U. Kevin, Rev. Prog. Quant. NDE. 6B (1987) 1175.